Performance Evaluation of a Hard Composite Solid Lubricant Coating when Dry Machining of High Carbon Steel

S. Gangopadhyay[1*], D. Bhaduri[2], A. K. Chattopadhyay[3], S. Paul[3]

[1]Department of Mechanical Engineering, National Institute of Technology Rourkela, Odisha, 769008, India

[2]Department of Mechanical Engineering, School of Engineering, University of Birmingham, Edgbaston, Birmingham, B15 2TT, UK

[3]Department of Mechanical Engineering, Indian Institute of Technology Kharagpur, West Bengal, 721302, India

*Corresponding author, Email: soumya.mech@gmail.com, soumyag@nitrkl.ac.in, Telephone: 0091-0661-2462528

Abstract

A novel hard composite solid lubricant coating, combining TiN and MoS_x, has been developed using pulsed DC closed-field unbalanced magnetron sputtering (CFUBMS). The tribological and mechanical properties together with their interdependencies with the coating microstructures have been assessed and published elsewhere. This paper evaluates the machining performance and correlates the underlying tribological aspects of different TiN-MoS_x coating architectures (deposited at titanium (Ti) cathode currents of 1, 3.5 and 5 A) when dry turning AISI 1080 high carbon steel. A comparative performance study clearly established the supremacy of the composite coating (deposited at 3.5 A Ti cathode current with ~12 wt% of

MoS_x) with a hard TiN underlayer over monolayer TiN, MoS_x and other related coating architectures in terms of cutting force, tool wear and workpiece surface roughness. The superlubricity behaviour of the said composite coated tool resulted in a reduction of cutting force (by up to ~45% compared to the uncoated tool) and exhibited a tool life of 8 min, which was 8 times and more than 2 times longer than that of the uncoated and conventional hard TiN coated counterparts, respectively. The workpiece surface roughness, R_a also decreased by 13 to 21% when machined with the TiN-MoS_x coated tool in comparison to the uncoated cemented carbide.

Keywords

Solid lubricant coating; magnetron sputtering; turning; cutting forces; tool wear; tool life.

INTRODUCTION

The development of functionally graded coatings, such as TiAlN, metal/carbon and TiN, using physical vapour deposition (PVD) for cutting tool applications has witnessed significant progress over the past three decades (Freller et al. (1), Lim et al. (2), (Bouzakis et al. (3)). The supremacy of PVD over chemical vapour deposition (CVD) was also established in a comprehensive study as the former process utilises lower operating temperatures and induces high compressive residual stresses within the coatings, thereby minimising the generation of irregular thermal cracks, as opposed to the latter technology (Venkatesh et al. (4)).

Although conventional hard coatings such as TiC, TiN, TiAlN, Al_2O_3 or other super hard coatings such as cBN and diamond have performed satisfactorily for machining a wide range of work materials, hard solid lubricant coatings, nowadays, have been assuming immense significance since they have the potential to promote environmental friendly dry machining or green manufacturing (Kustas et al. (5)). Derflinger et al. (6) commented that the deposition of a hard/lubricant coating on cutting tools could be a potential alternative to the extensive usage of cooling emulsion in metal cutting with benefits stemming from an improved chip flow characteristic with a lower coefficient of friction and reduced cutting force. Weinert et al. (7) argued that the lubricating function of the cutting fluids can be partly compensated by the soft 'self-lubricating' coatings such as MoS_2 or amorphous WC/C. Ideally, coated tools should possess high hot hardness, sufficient toughness, chemical inertness and high temperature stability. At the same time, it should also have good anti-friction or anti-sticking properties over a broad temperature range. Since it is neither feasible nor practical to expect all of these

properties from a single coating material, it is often required to combine the properties of two or more materials to achieve the desirable properties (Klocke and Krieg (8)). Klocke et al. (9) further remarked that complex stresses could be counteracted by combining various thin films in a multilayer fashion with improved coating-substrate adhesion and toughness properties.

Molybdenum disulphide (MoS_2) is a widely accepted solid lubricant coating that has been extensively used for components subject to friction and wear (Wang et al. (10), Luo et al. (11)). The super-lubricity behaviour of MoS_2 fostered its implementation in machining and the coating has been mainly employed in drilling and milling operations (Renevier et al. (12)). Rechberger and Dubach (13) showed that MoS_2 coated HSS end mills provided better workpiece surface finish and a two-fold higher productivity compared to the uncoated cemented carbide counterparts. However, owing to its low hardness and poor resistance to oxidation under humid environment, MoS_2 has been applied in machining either as a top coat with a hard underlayer (Settineri and Levi (14)) or as a multilayer (Kustas et al. (5)) or a non-multilayer composite coating (Teer et al. (15)). Further, MoS_x-based coatings could not be successfully implemented in turning steel materials due to the high machining temperatures encountered. Liu et al. (16) stated that MoS_2 coatings were not useful for all machining conditions; its effectiveness depended on the appropriate matching of cutting tools and workpieces that were related with the cutting temperature. MoS_x-Ti composite coating with hard underlayers such as TiC, TiCN and TiN could not exhibit any improvement in tool life compared to that obtained with the monolayer hard coatings when turning 34CrNiMo6 steel (Renevier et al. (17)). Deng et al. (18) and Song et al. (19) reported that MoS_x-Zr composite coated carbide turning tools led to a reduction in cutting force and improved tool life compared to those obtained with the uncoated

inserts when the cutting velocity was lower than 120 m/min. However, the same coating did not exhibit any improvement in performance at cutting velocities greater than 120 m/min. More recently, Ilyuschenko et al. (20) demonstrated that the drills coated with alternating layers of Chromium, nano-diamond and MoS_2-Cr were capable of restricting burr and built-up edge (BUE) formation and augmenting the tool life when machining $AlSi_9Cu_3$(Fe) aluminium alloy, in comparison to the uncoated counterparts. A minority of papers also detailed use of tungsten disulphide (WS_2) as a soft lubricating coating when dry turning of quenched and tempered AISI 1045 steel with results indicating reduction in cutting force and temperature at a high cutting speed of 200 m/min with respect to the uncoated carbide insert (Lian et al. (21)).

As it is well known that TiN is a versatile coating material for cutting tools with an excellent combination of hardness and toughness and is primarily suitable for machining steel, a few researchers have combined TiN with MoS_x and implemented the composite coating in drilling operations mainly but also in turning in limited cases. Goller et al. (22) reported a two-fold increase in tool life when drilling C35 steel with TiN+8 mol% MoS_x coated drills in comparison to the conventional TiN coating and up to five-fold higher tool life with respect to an uncoated drill. A 36% increase in drill lifetime was achieved when machining tool steel (DIN 1.2080) using TiN-MoS_x coated drills compared to the standard TiN (Cosemans et al. (23)). With the addition of a MoS_x top coating, the average tool life escalated by ~100%. It has been further shown that a similar composite coating exhibited improved tool life with respect to other coatings when turning alloy steels under liquid nitrogen environment (Jing et al. (24)).

An extensive research was undertaken by the authors on developing and characterising a novel TiN and MoS_x-based hard and wear resistant solid lubricant coating deposited by pulsed DC closed-field unbalanced magnetron sputtering (CFUBMS). The composite coating exhibited superior coating-substrate adhesion and better tribological properties compared to those for single layer TiN and MoS_x coatings (Gangopadhyay et al. (25)). Application of a hard TiN underlayer further augmented the properties of TiN-MoS_x by ensuring the higher load bearing capacity and better graduation of properties between the substrate and the TiN-MoS_x coating (Gangopadhyay et al. (25)). The tribological behaviour of the composite coatings deposited with different MoS_x content (weight%) as well as at different substrate bias voltages has also been evaluated and published elsewhere (Gangopadhyay et al. (26)-(28)). Some exploratory work by the authors exhibited superior performance of MoS_x-Ti (with a TiN underlayer) over uncoated cemented carbide when turning aluminium alloy and high carbon steel in terms of reducing the cutting force by ~9 to 17% and workpiece surface roughness by ~30 to 47% (Gangopadhyay et al. (29)). However, report on the potential of TiN-MoS_x composite coating in dry turning, which bears more significance in context to the industrial applicability for green manufacturing, is extremely limited. Therefore, the current investigation aimed at evaluating the performance of TiN-MoS_x composite coatings (deposited at different Ti cathode currents) with a TiN underlayer when dry turning of high carbon AISI 1080 steel and correlating the results with the underlying tribological properties. The effects of MoS_x concentration on the performance of TiN-MoS_x coated tools in terms of cutting force, tool wear and workpiece surface roughness were also studied. Furthermore, the performance of such composite coating system was compared with single layer TiN and MoS_x coatings together with other related coating architectures.

EXPERIMENTAL DETAILS

Deposition of coatings

ISO K10 grade cemented carbide (WC-6% Co) turning inserts (with ISO designation SNMA 12 04 08) were coated in a dual cathode physical vapour deposition (PVD) coating system utilising pulsed DC CFUBMS technique. TiN-MoS_x composite coatings were deposited by co-sputtering of Ti and MoS_2 targets in a mixture of Argon and Nitrogen atmosphere. Since the power to the MoS_2 target could not be changed over a wide range, the concentration of MoS_x in TiN-MoS_x coating was varied within the range of 30 to 6 wt% by selecting three different Ti cathode currents (I_{Ti}): 1, 3.5 and 5 A, see further details in Gangopadhyay et al. (26). However, in each case, a hard TiN underlayer of approximately 2 µm thickness was deposited prior to the co-deposition of TiN-MoS_x composite coating. The cathode current to the titanium and molybdenum disulphide targets was tuned gradually to the desired values in order to ensure a gradient interface. The scheme of all the coating architectures studied in the current investigation together with the corresponding average layer thicknesses are provided in Fig. 1. It is worth mentioning that a thin Ti interlayer with a thickness of ~100 nm was deposited directly onto the substrates prior to the deposition of functional coatings in order to promote better coating-substrate adhesion.

Turning tests

A comparative machining performance evaluation of the uncoated insert and the others coated with different architectures (as shown in Fig. 1) was carried out when dry turning AISI 1080 steel (with a hardness of 260 $HV_{0.5}$ and a tensile strength of 960 MPa). This particular

material is widely used in manufacturing different automotive parts, hand tools, springs and many other engineering components but is more difficult-to-machine than the low or medium carbon steels. All turning trials were carried out on a high speed precision lathe machine coupled with a range of spindle speed from 40 to 2040 rpm, and retrofitted with a frequency modulator in order to attain all levels of cutting velocity (V_c). The first phase of experiment (Phase 1) involved variation in V_c from 32 to 230 m/min but a constant feed rate (f) and depth of cut (a_e) of 0.2 mm/rev and 2 mm, respectively, with the aim of investigating the influence of cutting velocity on cutting forces for both uncoated and coated tools. The machining time in each trial was only 10 s during which axial (F_x) radial (F_y) and tangential (F_z) cutting forces were recorded using a KISTLER 9257B piezoelectric dynamometer. After 10 s of machining, the condition of the cutting tools was studied using optical microscopy, scanning electron microscopy (SEM) and energy dispersive X-ray spectroscopy (EDS). This was followed by the removal of built-up materials from the tool rake surfaces by dissolving them in an ultrasonic bath containing a solution of 20% concentrated H_2SO_4. The carbide inserts were then further examined using the optical microscopy, SEM and EDS. The average surface roughness (R_a) of the workpiece was measured using a contact based profilometer with a cut off length and evaluation length of 0.8 and 4 mm, respectively, as typically used for nearly all machined surfaces (Leech (30)). Three measurements were taken at different regions on the workpiece and the average value was calculated. Therefore, the strength and weakness of the coated and uncoated tools were ascertained from the cutting force data and degree of built-up edge (BUE) formation, particularly at a low cutting velocity.

Based on the results from Phase 1, two coated tools were selected for the tool life test in Phase 2: monolayer TiN coated insert (T2) and the tool coated with TiN-MoS_x (at I_{Ti} = 3.5 A) composite coating with a TiN underlayer (T7). Tool life test was also carried out for uncoated carbide insert (T1) in order to compare the performance of the coated tools with that of the uncoated one. All turning trials in Phase 2 were carried out under a dry environment at a constant cutting velocity of 200 m/min, feed rate of 0.2 mm/rev and depth of cut of 1.5 mm. After different intervals of machining, the conditions of the tools were monitored using optical microscopy and measurement of average flank wear (VB) until VB has reached the industrially accepted value of 0.3 mm. This was followed by examining the tools using the SEM and EDS.

RESULTS

Coating microstructure

Representative SEM images depicting the surface morphologies and fractographs of different coating architectures, in particular TiN, MoS_x over TiN, MoS_x-Ti over TiN, TiN-MoS_x (I_{Ti}: 3.5 A) and TiN-MoS_x (I_{Ti}: 3.5 A) over TiN are shown in Fig. 2. Evidently, the structure of the TiN-MoS_x was dense columnar with a smooth and dome-shaped morphology while the average grain size was smaller than that of the pure TiN and MoS_x-Ti coatings. The reduction in grain size in the former can be attributed to the competitive growth of both TiN and MoS_x phases in the co-deposited matrix. Conversely, growth kinetics of the MoS_x-Ti coating is slightly different with distortion of MoS_2 lattice due to the substitution of Mo atoms by Ti or formation of interstitial solid solution of MoS_x-Ti. This was possibly responsible for the absence of any columnar growth in the latter case (Teer et al. (15), Renevier et al. (12)). The structure and

properties of the other coating architectures were elaborately discussed in some previous work by the authors (Gangopadhyay et al. (25), (26)). The typical composite microhardness of the TiN-MoS_x coating deposited at I_{Ti}: 3.5 A (with an MoS_x content of around 12 wt%) was as high as 27 GPa (Gangopadhyay et al. (26)).

Phase 1: Comparative machining performance evaluation

The axial (F_x) and tangential forces (F_z) at different cutting velocities with various coated and uncoated tools are shown in Fig. 3. All turning inserts showed a decreasing trend in the force values, although in different degrees, as V_c increased from 32 to 230 m/min. It is also evident that the coated tools, except the one coated with pure MoS_x coating (tool T3), resulted in a considerable reduction in cutting force (up to ~45% compared to that recorded with the uncoated tool T1). Although a 12% decrease in F_x was observed for the tool T3 when machining with a V_c of 32 m/min, the same coated tool could not demonstrate any improvement in terms of reducing the cutting force at a velocity of 230 m/min, indicating a failure of the coating. The inability to retain pure MoS_x coating at the high cutting velocity could be attributed to its poor resistance to oxidation at elevated temperatures. A similar trend of variation was also observed for the tangential (F_z) and radial (F_y) components of cutting force; thus only the plot of F_z is shown in Fig. 3(b). No discerning change in the cutting force data was observed among the tools coated with TiN-MoS_x composite coatings with different MoS_x contents (tools T6 to T8) when machining at higher cutting velocities (130 and 230 m/min). However, the tool T7 coated with TiN-MoS_x (I_{Ti}: 3.5 A) with an MoS_x content of ~12 wt%, exhibited the minimum cutting force at low V_c, in particular 32 m/min. A better adhesion property obtained with this MoS_x content

compared to others (Gangopadhyay et al. (26)) might have caused improved retention of coating even at a reduced cutting velocity. It was further observed that the cutting forces recorded with all TiN-MoS_x coated tools (T6 to T8) have been consistently lower than those obtained with the tools coated with pure MoS_x or MoS_x-Ti coating with a TiN underlayer (T4 and T5 respectively). The superior performance of TiN-MoS_x composite coating can be attributed to the synergetic effect of TiN and MoS_x phases in the composite coating architecture. The TiN phase provided the necessary wear resistance and load bearing properties while the MoS_x ensured uninterrupted lubrication during the machining process. Similar argument was presented by Fortes Da Cruz (31) when assessing tribological and mechanical properties of WS_2 coating over a hard CrC underlayer.

Figure 4 shows optical images depicting the conditions of the rake surfaces for uncoated and different coated carbide inserts after machining at different cutting velocities. Pronounced material transfer from the chip to the uncoated tool rake surface (T1) was prevalent at a very low cutting velocity (32 m/min). However, material adhesion was considerably lower when V_c was increased to 77 m/min, although a trace of crater wear was observed on the rake surface after removal of the adhered material using sulphuric acid. The formation of built-up edge (BUE) was minimal when machining was conducted at further higher velocities of 130 and 230 m/min, albeit signs of crater wear appeared evidently on the rake surface within 10 s of machining, with increasing size and depth with the rise of V_c up to 230 m/min. This can be attributed to poor resistance to diffusion and wear of the uncoated K10 grade cemented carbide when machining steel, particularly at elevated cutting temperatures encountered at higher cutting velocities.

It was further observed from Fig. 4 that the MoS_x coating directly deposited on the WC tools (tool T3) or over a TiN underlayer (tool T4) suffered from premature wear of coating leading to the generation of built-up edge or built-up layer (BUL) at low cutting velocities. Although such tool failures were diminished with the increase of V_c, coating oxidation and crater wear formation at higher cutting speeds could not be avoided. Molybdenum disulphide doped with metal (Ti) or metallic nitrides (TiN) at low and high Ti cathode current (1 A and 5 A) also did not improve the scenario of coating delamination and subsequent BUL on tools T5, T6 and T8 respectively, when machining at 32 and 77 m/min. However, these signals of tool wear together with the formation of crater considerably decreased at higher cutting speeds of 130 and 230 m/min. In contrast, single layer TiN (tool T2) and TiN-MoS_x deposited at 3.5 A Ti target current (tool T7) exhibited minimal signs of tool wear throughout the range of cutting velocity tested.

With a view to achieve a deeper insight to the wear mechanism and material transfer during machining, SEM images together with the EDS spectra at the chip-tool interaction zone corresponding to the lowest (32 m/min) and highest (230 m/min) cutting velocities are demonstrated in Fig. 5. Severe material adhesion on the uncoated insert at low cutting velocities was apparent (Fig. 5(a)). Conversely, TiN-MoS_x composite coating was capable of successfully restricting the chip adhesion to the tool rake face and crater wear even at a high cutting velocity of 230 m/min, see Fig. 5(b). However, some amount of material adhesion on the cutting edge was observed in the SEM image which was further confirmed using EDS as shown in Fig. 5(a). The optical and SEM micrographs further revealed that the chip-tool contact length decreased with an increase of cutting velocity. Additionally, the contact length for TiN as well as TiN-

MoS_x composite coated tools was shorter compared to that for the uncoated tool T1, due to the reduction in chip-tool interface friction.

Figure 6 shows EDS mapping images of tool T4 (MoS_x over a TiN underlayer) after machining at 77 m/min followed by the removal of built-up material. It was noticed that the spallation of coating from the rake surface fostered material build-up at lower cutting velocities. Therefore, the ability to retain the TiN-MoS_x (tools T6, T7 and T8) and monolayer TiN (tool T2) coatings even at low V_c can possibly explain the lower cutting forces recorded with these tools, in comparison to that obtained with the other coated inserts.

The conditions of rake surface of the uncoated (T1) and other coated tools (T2 to T8) after machining for 10 s at the highest V_c (230 m/min) and subsequent BUL removal are shown in Fig. 7. While the uncoated tool (T1) resulted in a large crater depth within a short duration of machining due to the inferior resistance to diffusion, the other coated tools, with the exception of tool T3 (coated with single layer MoS_x), showed improved resistance to crater wear at higher cutting velocities. Especially, coating defects/damages were negligible in the TiN (T2) and TiN-MoS_x (T6, T7 and T8) coated tools.

The workpiece average surface roughness (R_a) measured following machining with different coated and uncoated tools is shown in Fig. 8. As expected, R_a typically decreased with the increase of cutting velocity. With the exception of machining trials at 77 m/min, the uncoated tool generally exhibited the maximum surface roughness values (1.9 to 2.2 µm) amongst all the coated tools. Although the workpiece roughness obtained following turning with tools T2, T4 and T6 was comparable, tool T7 rendered the best surface finish with R_a varying between 1 to

1.7 µm. This was in agreement with the trend of cutting force data recorded with these coated inserts. The superlubricity of $MoS_{x,}$ doped with a hard TiN phase, might have resulted in lower frictional force, leading to an improved work surface quality.

Phase 2: Tool life test

The promising machining behaviour (in terms of cutting force and tool wear) of the conventional TiN coated (T2) and TiN-MoS_x coated (T7, I_{Ti}: 3.5 A, with an MoS_x content of ~12 wt% and a TiN underlayer) tools throughout the entire range of cutting velocity, fostered further study on tool life testing in Phase 2. The uncoated cemented carbide tool (T1) was also tested for the purpose of comparison. Figure 9 reveals the condition of rake and flank surfaces of these tools after 30 and 60 s of machining. Evidently, the growth of crater and flank wear for the uncoated insert was much faster with a tool life only limited to 60 s of machining. Conversely, both TiN (T2) and TiN-MoS_x coated tools (T7) exhibited significant influence in restricting the crater and flank wear. However, with the progress of machining, growth rate of tool T7's flank wear was much slower than that of tool T2. TiN coated insert (T2) reached the end of its tool life after 210 s, whereas TiN-MoS_x coated tool (T7) demonstrated a gradual increase of flank wear up to 0.3 mm after 480 s of machining. Hence, the tool life of T7 was 8 times and more than 2 times longer than that of the uncoated and conventional hard TiN coated counterparts, respectively, which is graphically depicted in Fig. 10.

DISCUSSION

The design of multilayer coating system with the combination of coating materials having high and low elastic moduli permits sliding within the layers and lower bending stress ensuring

"long bending strain to failure." As a result, the ratio of hardness (H) to elastic modulus (E) of a multilayer coating is higher than the monolayer hard coating. Shear deformation takes place at the soft phase so that the thinner hard layer does not experience high bending stresses. This protects the hard coating from failure due to fracture, delamination and fatigue (Matthews et al. (32), Matthews et al. (33)). The theoretical model developed by Nyqvist et al. (34) predicts the contact pressure, real areas of contact and a complete subsurface stress field for multilayer contacts. It has been observed that single layer hard coating induces detrimental tensile stress at the chip-tool interface and within the coating during tribological interaction. This can be mitigated by adopting multilayer coatings that causes more favourable stress distribution within the coating compared to the monolithic counterparts with equivalent coating thickness. The higher adhesion strength and crack / wear resistance of multilayer coatings are due to the rotation of columnar grains and crack deflection of interlayer thickness length scale, respectively (Roa et al. (35)).

Previous work by the authors showed that TiN-MoS_x composite coatings deposited with or without a TiN underlayer exhibited 9-25% higher critical loads, in the range of 60 to 65 N, in scratch adhesion tests compared to monolithic TiN or MoS_x layers (Gangopadhyay et al. (25)). The tool T7 coated with an MoS_x content of ~12 wt% thus exhibited minimum film spallation in high speed turning due to superior coating-substrate adhesion with respect to the other coated inserts. The performance of T7 was further augmented due to its improved friction and load bearing characteristics stemming from the sufficiently high microhardness ($HV_{0.005}\approx$ 27 GPa) of the combined TiN-MoS_x coating (Gangopadhyay et al. (26)). A further increase in MoS_x content (30 wt%) resulted in reduction of both critical load (43 N) and microhardness (~15 GPa) which

was translated in the inferior performance of tool T6 in machining. The results further demonstrated that these coating properties controlled the wear coefficient in pin-on-disc tribological tests. While the coating on T7 showed wear coefficient as low as 5×10^{-16} m^3/Nm, those on T6 and T8 exhibited wear rates of 1.2×10^{-15} and 2.6×10^{-15} m^3/Nm, respectively. Similar observation was also reported by Braic et al. (36) when evaluating the wear rate of multilayered TiSiC/NiC coatings. The excellent anti-adhesive behaviour of tool T7 at low cutting velocities was also fostered by the superlubricity of MoS_x in TiN-MoS_x that was caused by the adaptation of the coating to the intense friction conditions (Fox-Rabinovich et al. (37)) by forming MoO_3, acting as a solid lubricant in the machining zone (Sergevnin et al. (38)). The argument is supported by Fig. 11 that shows superlubricity behaviour of the TiN-MoS_x coating with a coefficient of friction at the order of 0.04, much lower than that of the conventional TiN (~0.6 to 0.7). Data in Fig. 11 have been extracted from (Gangopadhyay et al. (25) and (26)). Hence, it can be inferred that the synergistic effect of high critical load with adequate microhardness and superlubricating properties of TiN-MoS_x coating has been sincerely reflected in the performance of tool T7 in terms of restricting both abrasive and adhesive wear when machining under aggressive cutting conditions.

CONCLUSIONS

A novel hard solid lubricant coating combining the properties of TiN and MoS_x was developed and deposited on cemented carbide inserts using pulsed DC CFUBMS technique. The performance evaluation of the carbide tools coated with various composite coating architectures was carried out in dry turning of high carbon steel in comparison with uncoated and other

monolithic coated tools. Monolayer TiN and TiN-MoS_x composite coating (with MoS_x content of ~12 wt% and a TiN underlayer) successfully restricted the formation of built-up edge at a low cutting velocity of 32 m/min and consequently resulted in a significant reduction in cutting forces (by up to ~45%). The latter further proved its efficiency in arresting the crater wear at higher cutting velocities such as 130 and 230 m/min while rendering the best work surface quality with a 13 to 21% reduction in R_a compared to the uncoated insert. During the tool life test, the tool coated with the said hard solid lubricant composite coating exhibited an 8 times higher tool life than that of the uncoated and more than 2 times longer tool life compared to that of the conventional hard TiN coated counterparts when machining at a cutting velocity of 200 m/min, feed rate of 0.2 mm/rev and depth of cut of 1 mm. The developed coated tool therefore demonstrated a strong promise towards achieving the eco-friendly machining of difficult-to-cut materials under dry or near dry environment.

ACKNOWLEDGEMENTS

The authors sincerely acknowledge the funding received from DST, FIST (Sanction No. SR / FST / ET -- II -- 003 / 2000 dated 20.5.2002), Ministry of Human Resource Development, Government of India (Project code: MCS, Sanction No. F.26-14/2003-TS.V dated 14-01-2004). The authors are also thankful to Dr. N.C. Pant, former Professor of Department of Geology and Geophysics, IIT Kharagpur, India, for providing the SEM and EDS facilities.

REFERENCES

(1) Freller, H., Günther, K.G., Hässler, H., and Siemens, A.G. (1988), "Progress in physical vapour deposited wear resisting coatings on tools and components," CIRP Annals - Manufacturing Technology, **37**(1), pp 165-169.

(2) Lim, C.Y.H., Lim, S.C., and Lee, K.S. (1999), "The performance of TiN-coated high speed steel tool inserts in turning," Tribology International, **32**, pp 393-398.

(3) Bouzakis, K.-D., Michailidis, N., Vidakis, N., Eftathiou, K., Kompogiannis, S., and Erkens, G. (2000), "Interpretation of PVD coated inserts wear phenomena in turning," CIRP Annals - Manufacturing Technology, **49**(1), pp 65-68.

(4) Venkatesh, V.C., Ye, C.T., Quinto, D.T., and Hoy, D.E.P. (1991), "Performance studies of uncoated, CVD-coated and PVD-coated carbides in turning and milling," CIRP Annals - Manufacturing Technology, **40**(1), pp 545-550.

(5) Kustas, F.M., Fehrehnbacher, L.L., and Komanduri, R. (1997), "Nanocoatings on cutting tools for dry machining," CIRP Annals - Manufacturing Technology, **46**(1), pp 39**-**42.

(6) Derflinger, V., Brändle, H., and Zimmermann, H. (1999), "New hard/lubricant coating for dry machining," Surface and Coatings Technology, **113**, pp 286-292.

(7) Weinert, K., Inasaki, I., Sutherland, J.W., and Wakabayashi, T. (2004), "Dry machining and minimum quantity lubrication," CIRP Annals - Manufacturing Technology, **53**(2), pp 511-537.

(8) Klocke, F. and Krieg, T. (1999), "Coated tools for metal cutting – features and applications," CIRP Annals - Manufacturing Technology, **48**(2), pp 515-525.

(9) Klocke, F., Krieg, T., Gerschwiler, K., Fritsch, R., Zinkann, V., Pöhls, M., and Eisenblätter, G. (1998), "Improved cutting processes with adapted coating systems," CIRP Annals - Manufactruing Technology, **47**(1), pp 65-68.

(10) Wang, Fu-Xing, Wu, Yun-Xin, Cheng Yin-Qian, Wang, B., and Danyluk, S. (2008), "Effects of solid lubricant MoS_2 on the tribological behavior of hot-pressed Ni/MoS_2 self-lubricating composites at elevated temperatures," Tribology Transactions, **39**(2), pp 392-397.

(11) Luo, J., Cai, Z.B., Mo, J.L., Peng, J.F., and Zhu, M.H. (2015), "Torsional fretting wear behavior of bonded MoS_2 solid lubricant coatings," Tribology Transactions, **58**(6), pp 1124-1130.

(12) Renevier, N.M., Lobiondo, N., Fox, V.C., Teer, D.G., and Hampshire, J. (2000), "Performance of MoS_2/metal composite coatings used for dry machining and other industrial applications," Surface and Coatings Technology, **123**, pp 84-91.

(13) Rechberger, J., and Dubach, R. (1993), "Soft physical vapour deposition coatings–a new coating family for high performance cutting tools," Surface and Coatings Technology, **60**, pp 584-586.

(14) Settineri, L., and Levi, R. (2005), "Surface properties and performance of multilayer coated tools in turning Inconel," CIRP Annals - Manufacturing Technology, **54**(1), pp 515-518.

(15) Teer, D.G., Hampshire, J., Fox, V., and González, V.B. (1997), "The tribological properties of MoS_2/metal composite coatings deposited by closed field magnetron sputtering," Surface and Coatings Technology, **94/95**, pp 572-577.

(16) Liu, Y.-R., Liu, J.-J., and Du, Z. (1999), "The cutting performance and wear mechanism of ceramic cutting tools with MoS_2 coating deposited by magnetron sputtering," Wear, **231**, pp 285-292.

(17) Renevier, N.M., Oosterling, H., König, U., Dautzenberg, H., Kim, B.J., Geppert, L., Koopmans, F.G.M., and Leopold, J. (2003), "Performance and limitations of MoS_2/Ti composite coated inserts," Surface and Coatings Technology, **172**, pp 13-23.

(18) Deng, J., Song, W., Zhang, H., and Zhao, J. (2008), "Performance of PVD MoS_2/Zr-coated carbide in cutting processes," International Journal of Machine Tools and Manufacture, **48**, pp 1546-1552.

(19) Song, W., Deng, J., Zhang, H., and Yan, P. (2010), "Study on cutting forces and experiment of MoS_2/Zr-coated cemented carbide tool," Interanational Journal of Advanced Manufacturing Technology, **49**, pp 903-909.

(20) Ilyuschenko, A.P., Feldshtein, E.E., Lisovskaya, Y.O., Markova, L.V., Andreyev, M.A., Albert, and Lewandowski, A. (2015), "On the properties of PVD coating based on

nanodiamond and molybdenum disulfide nanolayers and its efficiency when drilling of aluminum alloy," Surface and Coatings Technology, **270**, pp 190-196.

(21) Lian, Y., Deng, J., Li, S., Xing, Y., and Chen, Y. (2013), "Preparation and cutting performance of WS_2 soft-coated tools," Interanational Journal of Advanced Manufacturing Technology, **67**(5-8), pp 1027-1033.

(22) Goller, R., Torri, P., Baker, M.A., Gilmore, R., and Gissler, W. (1999), "The deposition of low-friction TiN-MoS_x hard coatings by a combined arc evaporation and magnetron sputter process," Surface and Coatings Technology, **120/121**, pp 453-457.

(23) Cosemans, P., Zhu, X., Celis, J.P., and Van Stappen, M. (2003), "Development of low friction wear-resistant coatings," Surface and Coatings Technology, **174/175**, pp 416-420.

(24) Jing, Y., Luo, J., and Pang, S. (2004), "Effect of Ti or TiN codeposition on the performance of MoS_2-based composite coatings," Thin Solid Films, **461**, pp 288-293.

(25) Gangopadhyay, S., Acharya, R., Chattopadhyay, A.K., and Paul, S. (2009), "Pulsed DC magnetron sputtered MoS_x–TiN composite coating for improved mechanical properties and tribological performance," Surface and Coatings Technology, **203**, pp 3297-3305.

(26) Gangopadhyay, S., Acharya, R., Chattopadhyay, A.K., and Paul, S. (2009), "Composition and structure-property relationship of low friction, wear resistant TiN-MoS_x composite coating deposited by pulsed closed-field unbalanced magnetron sputtering," Surface and Coatings Technology, **203**, pp 1565-1572.

(27) Gangopadhyay, S., Acharya, R., Chattopadhyay, A.K., and Paul, S. (2010), "Effect of substrate bias voltage on structural and mechanical properties of pulsed DC magnetron sputtered TiN–MoS_x composite coatings," Vacuum, **84**(6), pp 843-850.

(28) Gangopadhyay, S., Acharya, R., Chattopadhyay, A.K., and Paul, S. (2010), "Effects of Deposition Conditions and Counter Bodies on the Tribological Properties of Pulsed DC Magnetron Sputtered TiN–MoS_x Composite Coating," Tribology Letters, **37**(3), pp 487-496.

(29) Gangopadhyay, S., Acharya, R., Chattopadhyay, A.K., and Paul, S. (2010), "On deposition and characterisation of MoS_x-Ti multilayer coating and performance evaluation in dry turning of aluminium alloy and steel," *Proceedings of 36th International MATADOR Conference*: Manchester, UK, pp 247-250.

(30) Leech, R. (2001), "Measurement Good Practice Guide No. 37, The Measurement of Surface Texture using Stylus Instruments," National Physical Laboratory, UK, ISBN 1368-6550.

(31) Fortes Da Cruz, J., Da Silva Botelho, T., Lemaire-Caron, I., Durand, A-M., and Messager, D. (2016), "Role of WS_2, WS_2 + CrC and bonded coatings on damage and friction of Inconel 718 flat rough surfaces at high temperature," Tribology International, **100**, pp 430-440.

(32) Matthews, A., Jones, R., and Dowey, S. (2001), "Modelling the deformation behaviour of multilayer coatings," Tribology Letters, **11**(2), pp 103-106.

(33) Matthews, A., Franklin, S., and Holmberg, K. (2007), "Tribological coatings: contact mechanisms and selection," Journal of Physics D: Applied Physics, **40**, pp 5463-5475.

(34) Nyqvist, J., Kadiric, A., Ioannides, S., and Sayles, R. (2015), "Semi-analytical model for rough multilayered contacts," Tribology International, **87**, pp 98-112.

(35) Roa, J.J., Jiménez-Piqué, E., Martínez, R., Ramírez, G., Tarragó, J.M., Rodríguez, R., and Llanes, L. (2014), "Contact damage and fracture micromechanisms of multilayered TiN/CrN coatings at micro- and nano-length scales," Thin Solid Films, **571**, pp 308-315.

(36) Braic, M., Balaceanu, M., Parau, A.C., Dinu, M., and Vladescu, A. (2015), "Investigation of multilayered TiSiC/NiC protective coatings," Vacuum, **120**, pp 60-66.

(37) Fox-Rabinovich, G.S., Yamamoto, K., Kovalev, A.I., Veldhuis, S.C., Ning, L., Shuster, L.S., and Elfizy, A. (2008), "Wear behavior of adaptive nano-multilayered TiAlCrN/NbN coatings under dry high performance machining conditions," Surface and Coatings Technology, **202**, pp 2015-2022.

(38) Sergevnin, V.S., Blinkov, I.V., Volkhonskii, A.O., Belov, D.S., Kuznetsov, D.V., Gorshenkov, M.V., and Skryleva, E.A. (2016), "Wear behaviour of wear-resistant adaptive nano-multilayered Ti-Al-Mo-N coatings" Applied Surface Science, **388**, pp 13-23.

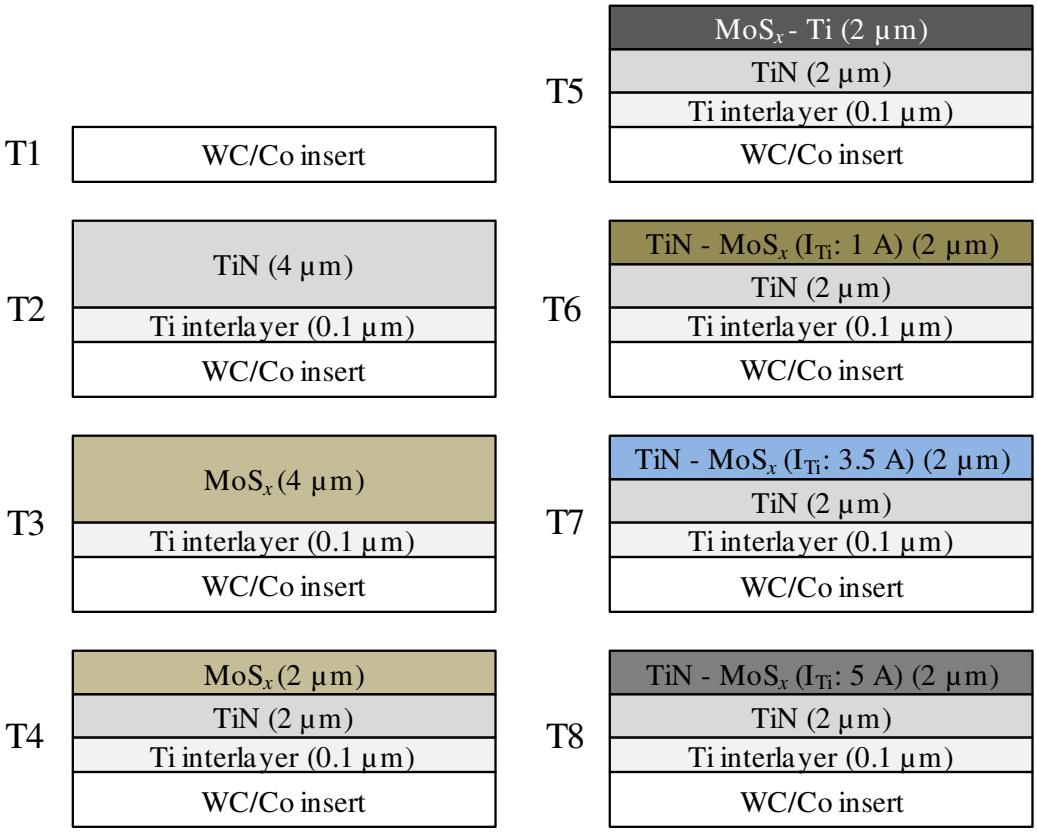

Fig. 1 Different coating architectures and the corresponding layer thicknesses deposited on tungsten carbide inserts; T1: Uncoated, T2-T8: coated

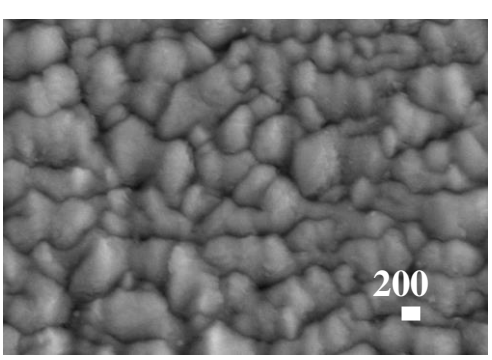

(a)

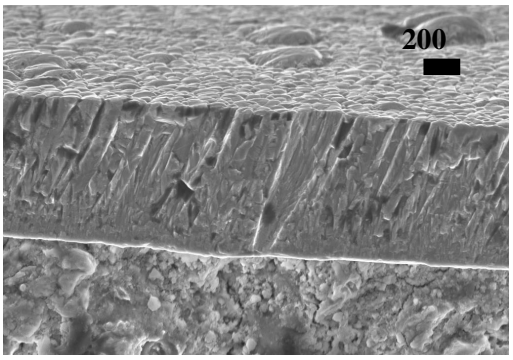

(b)

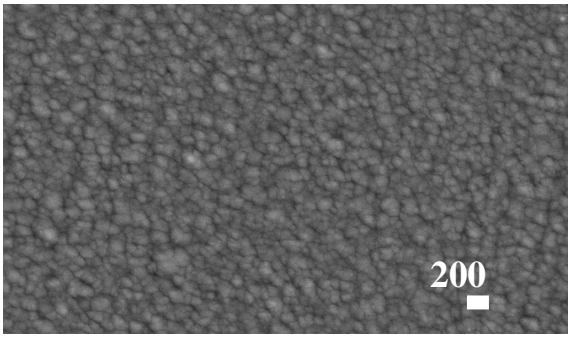

(c)

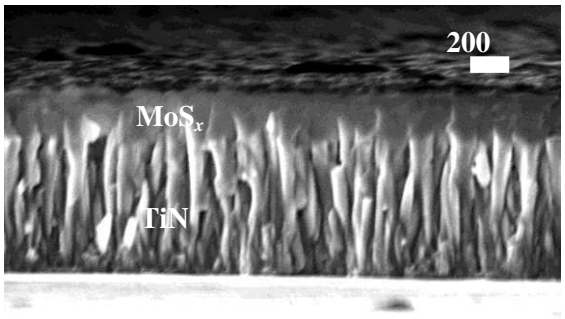

(d)

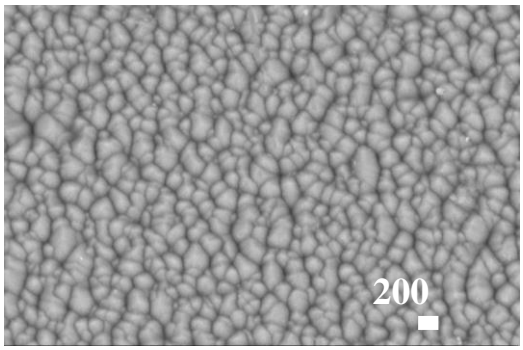

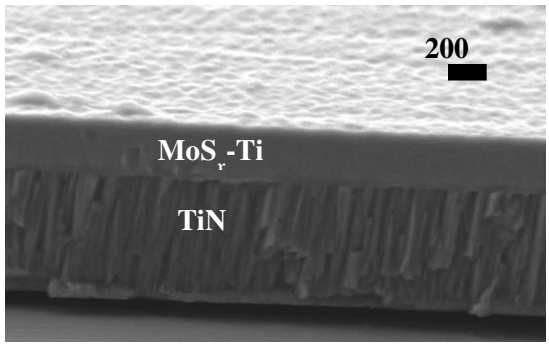

(e) (f)

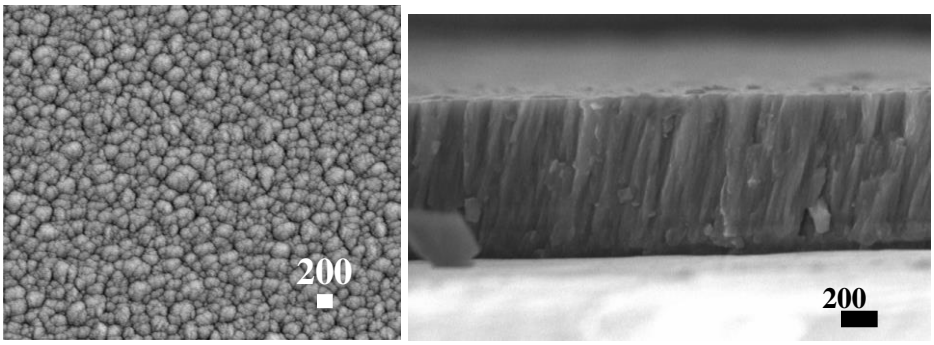

(g) (h)

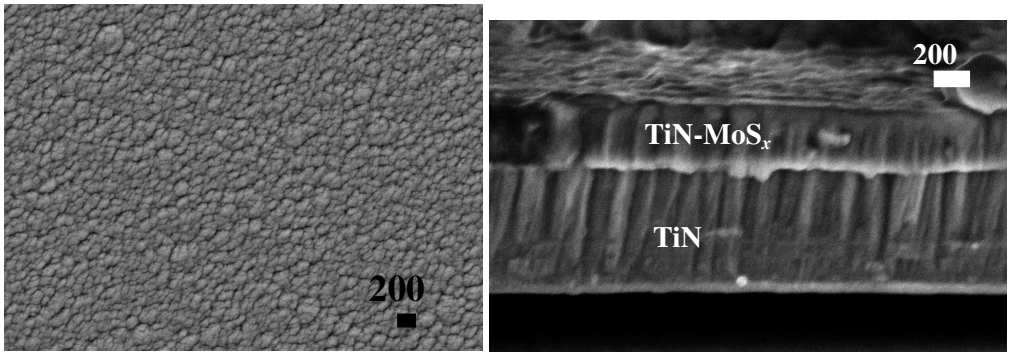

(i) (j)

Fig. 2 SEM images of respective surface morphologies and fractured cross-sections of (a)-(b) TiN, (c)-(d) MoS_x over TiN, (e)-(f) MoS_x-Ti over TiN, (g)-(h) TiN-MoS_x (I_{Ti}: 3.5 A) and (i)-(j) TiN-MoS_x (I_{Ti}: 3.5 A) over TiN

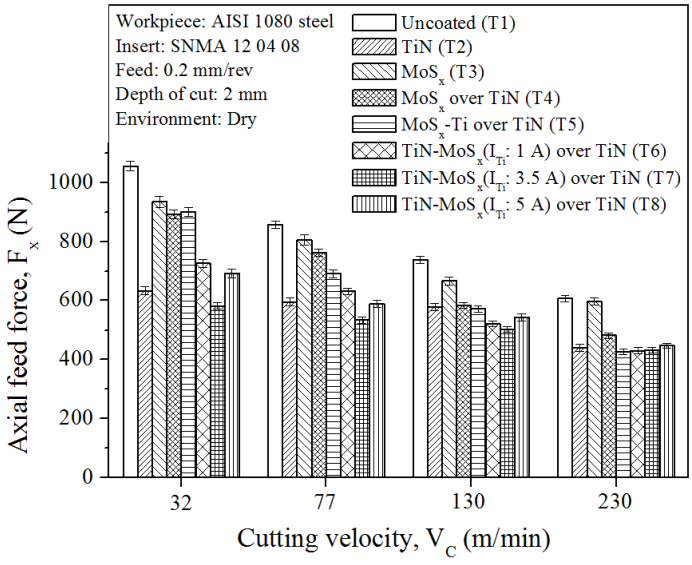

(a)

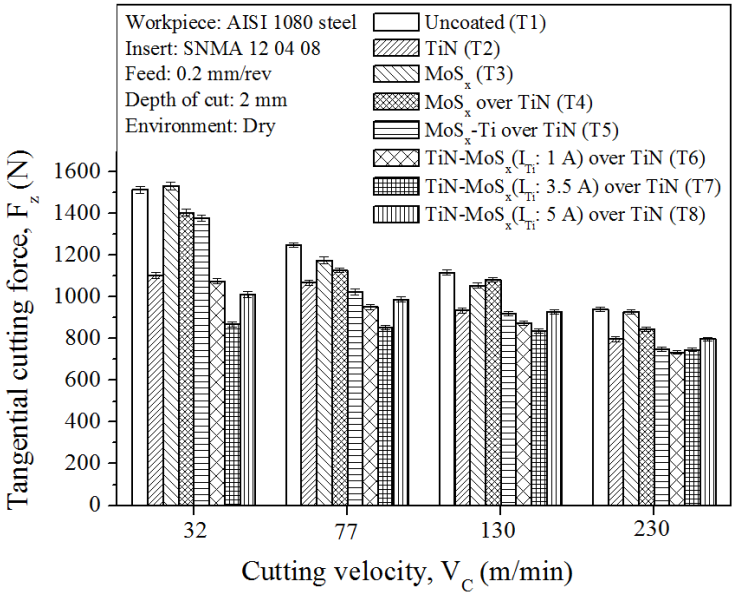

(b)

Fig. 3 Variation of (a) axial force and (b) tangential cutting force against cutting velocity when machining with uncoated and different coated turning inserts

Workpiece: AISI 1080 steel, f: 0.2 mm/rev, a_e: 2 mm, Environment: Dry				
Cutting tools	Cutting velocity(V_c),m/min			
	32	77	130	230
Uncoated (T1)	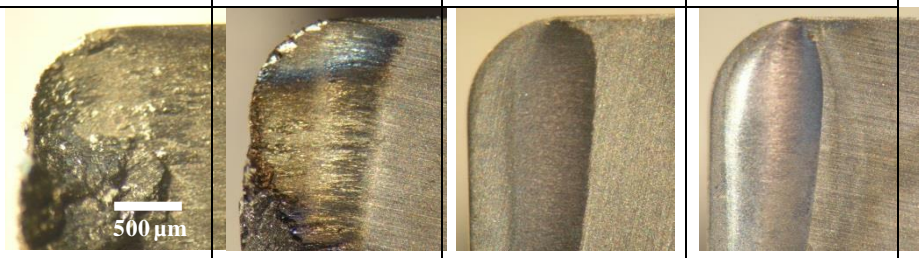			
TiN (T2)	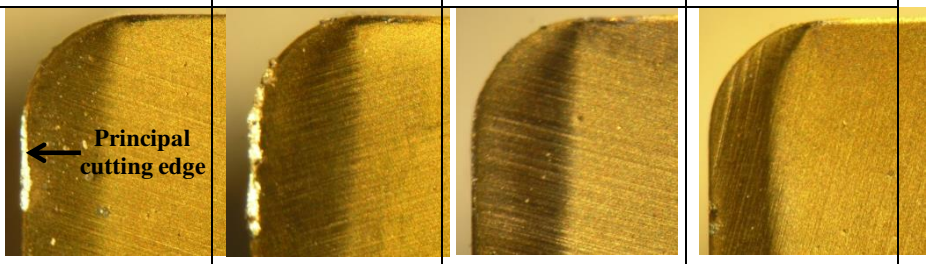			
MoS_x (T3)	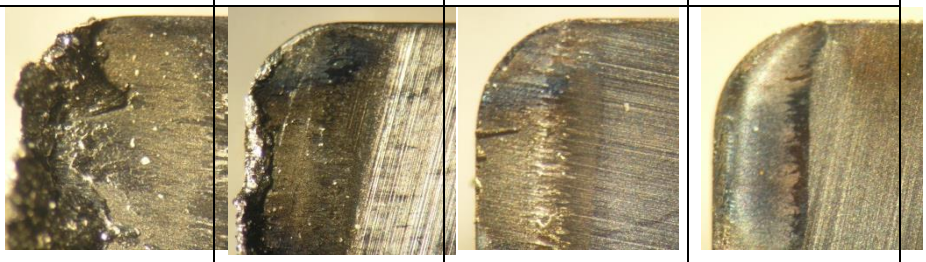			
MoS_x over TiN (T4)	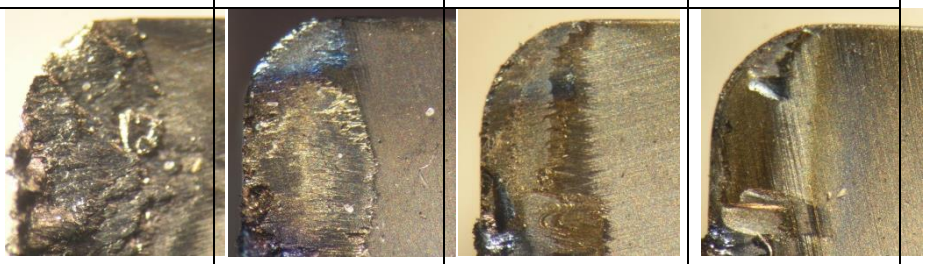			
MoS_x-Ti over TiN (T5)	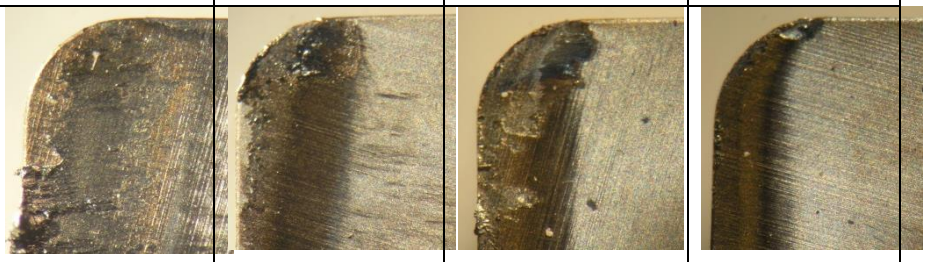			

Cutting tools	Cutting velocity (V_c), m/min			
	32	77	130	230
TiN-MoS_x (I_{Ti}: 1A) over TiN (T6)	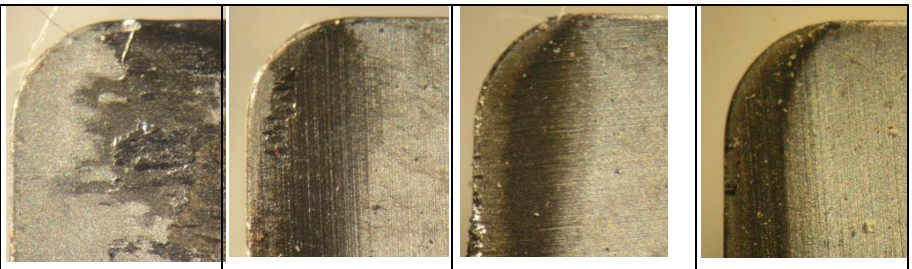			
TiN-MoS_x (I_{Ti}: 3.5A) over TiN (T7)	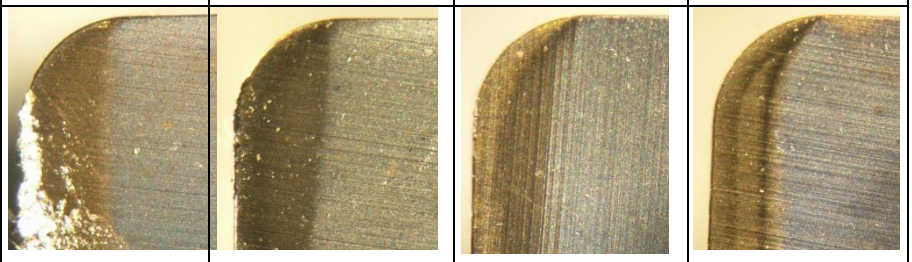			
TiN-MoS_x (I_{Ti}: 5A) over TiN (T8)	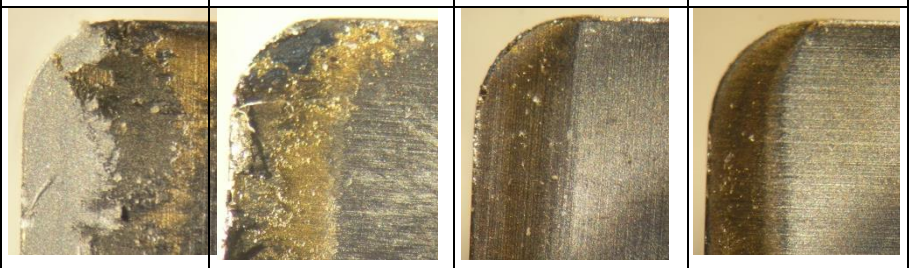			

Fig. 4 Optical micrographs (with 20X magnification) of the rake surface of uncoated and different coated inserts after 10 s of machining at different cutting velocities

Workpiece: AISI 1080 steel, V_c: 32 m/min, f: 0.2 mm/rev, a_e: 2 mm, Environment: Dry		
Cutting tools	SEM images	EDS spectra
Uncoated (T1)	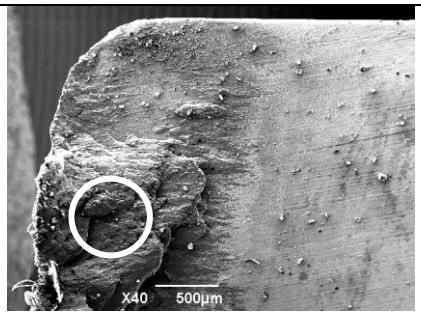	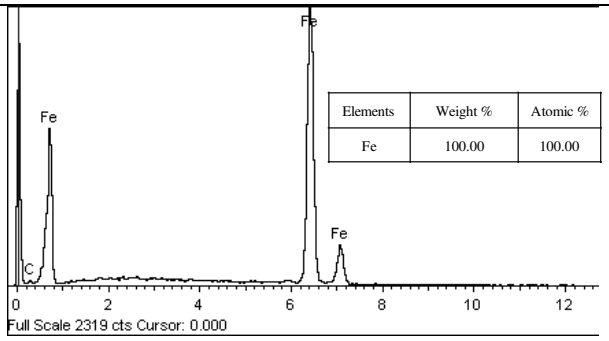
TiN (T2)	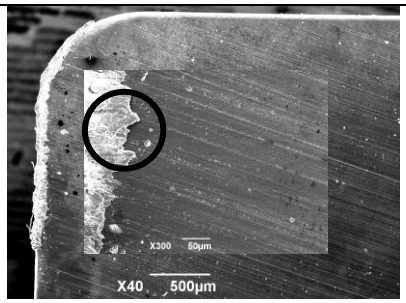	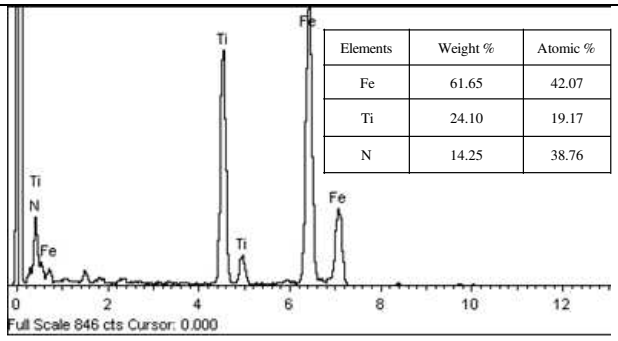
TiN-MoS_x (I_{Ti}: 3.5A) over TiN (T7)	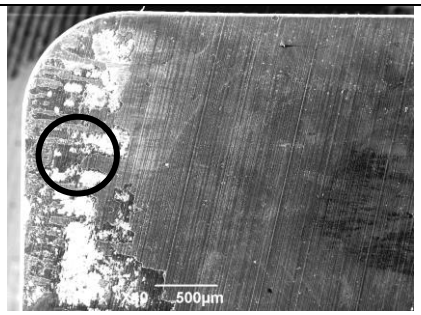	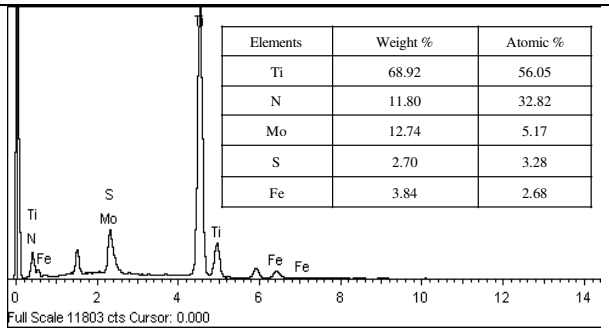

Elements	Weight %	Atomic %
Fe	100.00	100.00

Elements	Weight %	Atomic %
Fe	61.65	42.07
Ti	24.10	19.17
N	14.25	38.76

Elements	Weight %	Atomic %
Ti	68.92	56.05
N	11.80	32.82
Mo	12.74	5.17
S	2.70	3.28
Fe	3.84	2.68

(a)

Workpiece: AISI 1080 steel, V_c: 230 m/min, f: 0.2 mm/rev, a_e: 2 mm, Environment: Dry

Cutting tools	SEM images	EDS spectra
Uncoated (T1)	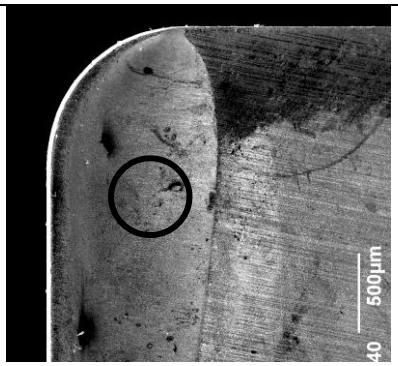	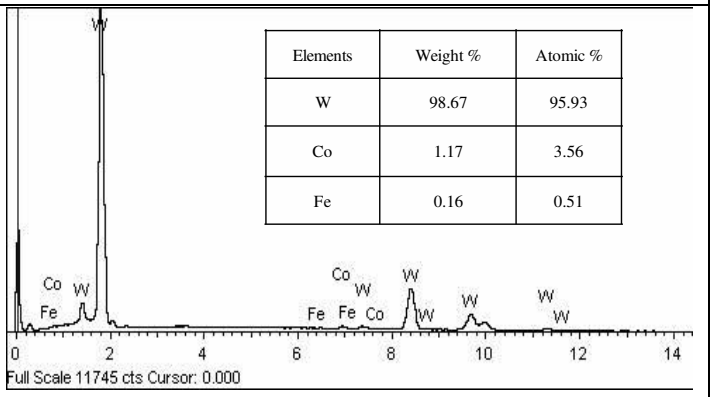
TiN (T2)	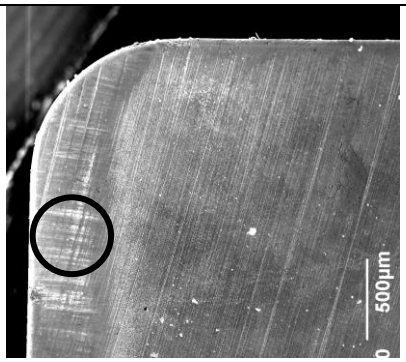	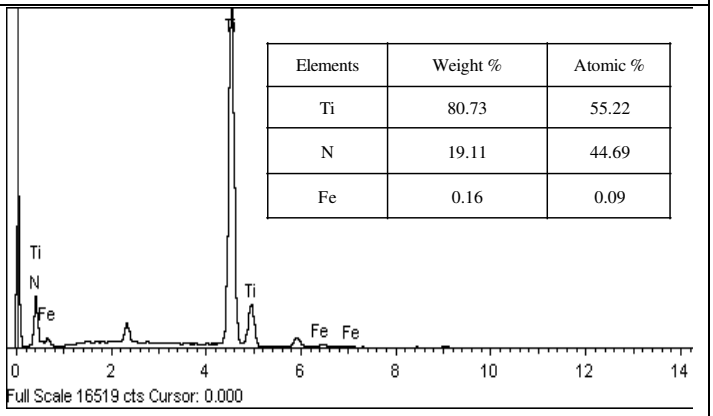
TiN-MoS_x (I_{Ti}: 3.5A) over TiN (T7)	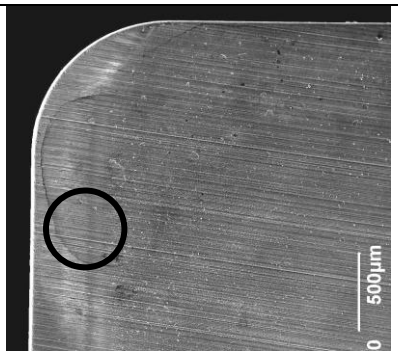	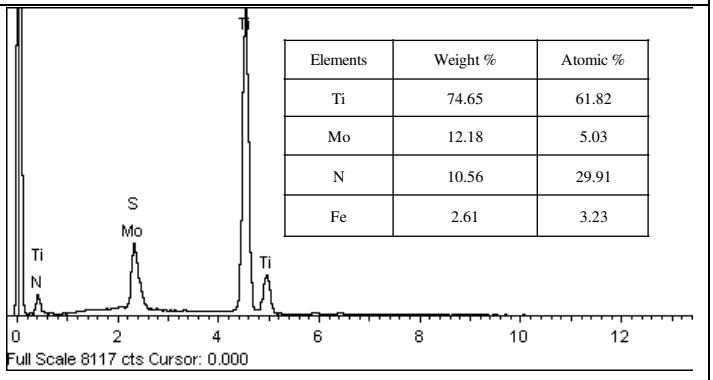

(b)

Fig. 5 SEM micrographs together with the EDS spectra of uncoated and different coated tools after 10 s of machining at cutting velocities of (a) 32 m/min. and (b) 230 m/min

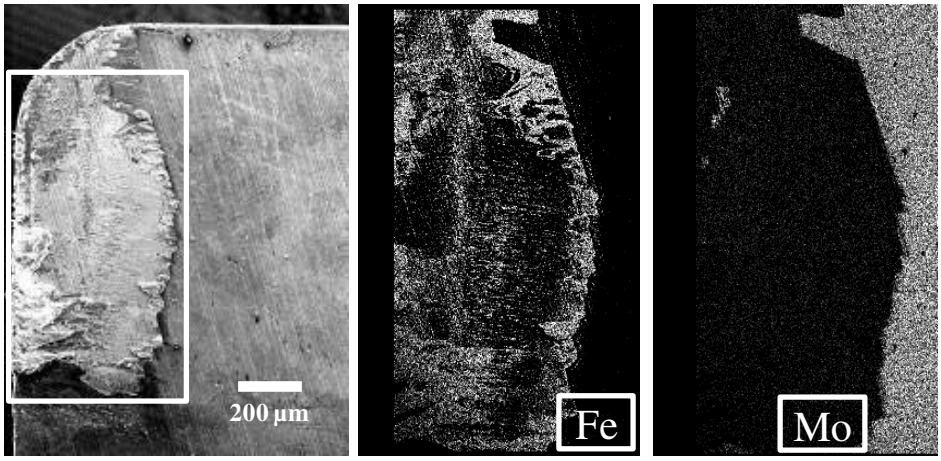

(a)

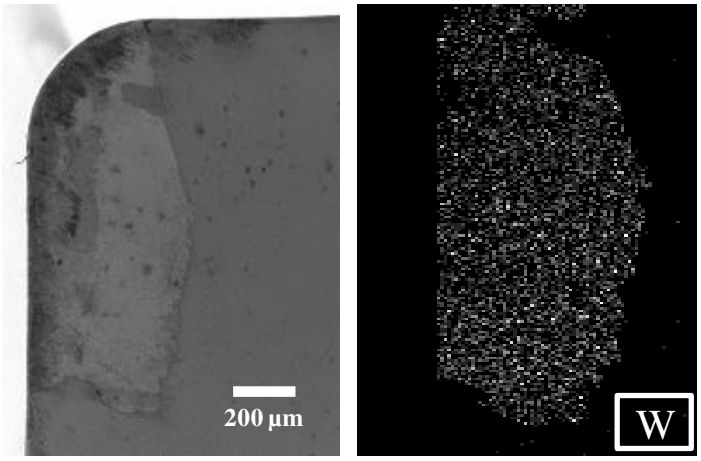

(b)

Fig. 6 EDS mapping of MoSx coated tool with TiN underlayer (T4) after machining: (a) before and (b) after removal of built-up layer (machining conducted at V_c= 77 m/min, f= 0.2 mm/rev, a_e= 2 mm)

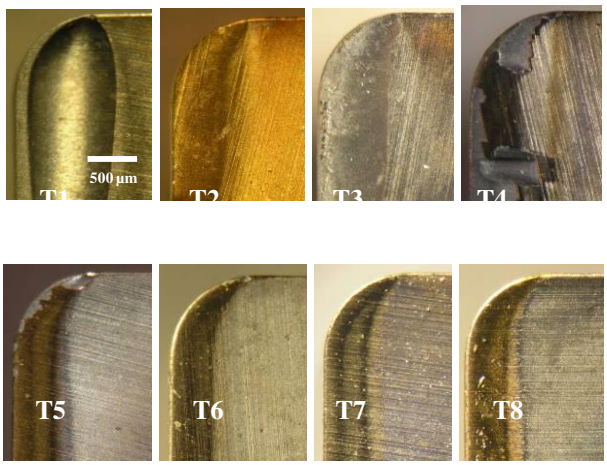

Fig. 7 Optical micrographs of the rake surface of uncoated (T1) and different coated turning inserts (T2 to T8) after machining (V_c= 230 m/min, f= 0.2 mm/rev, a_e= 2 mm) followed by the removal of built-up material

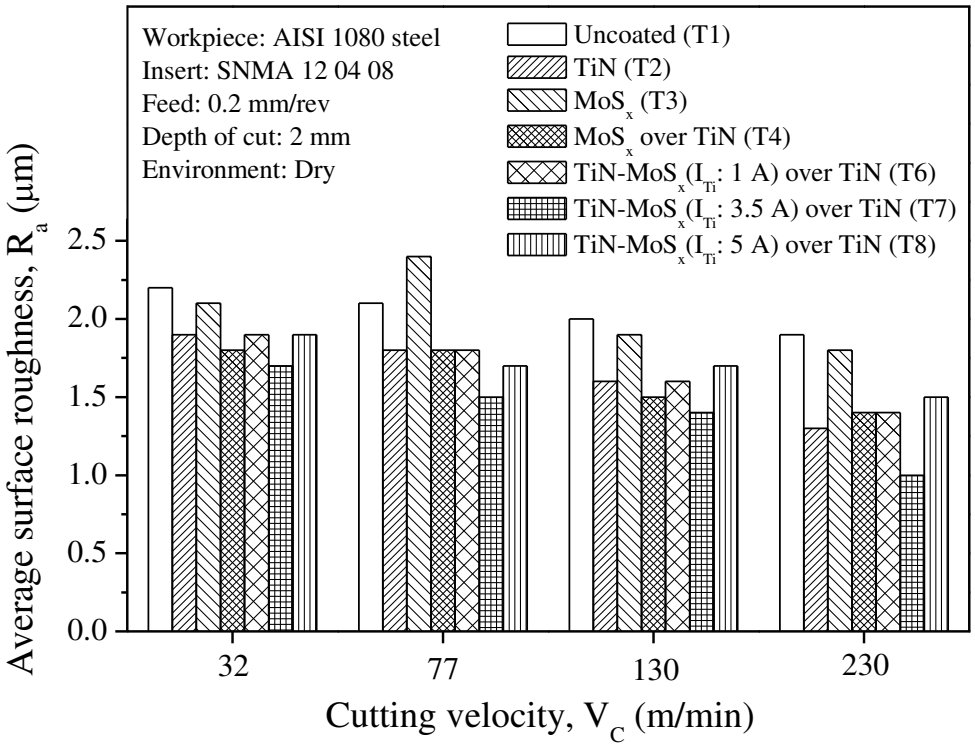

Fig. 8 Workpiece average surface roughness (R_a) measured following machining with different coated and uncoated tools

Machining duration	Workpiece: AISI 1080 steel, V_c: 200 m/min, f: 0.2 mm/rev, a_e: 1.5 mm, Environment: Dry			
		T1	T2	T7
30 s	Rake	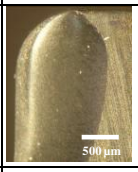	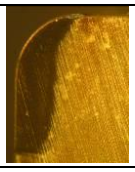	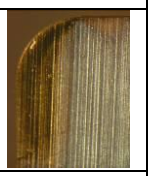
	Flank		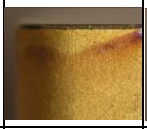	
60 s	Rake		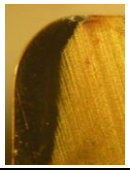	
	Flank		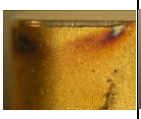	
180 s	Rake		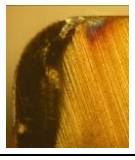	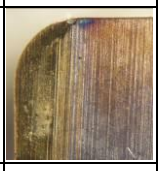
	Flank		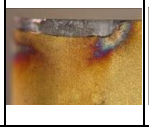	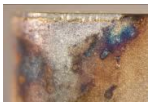

Fig. 9 Optical micrographs of rake and flank surfaces of the uncoated (T1), TiN coated (T2) and TiN-MoS_x (I_{Ti}: 3.5 A) coated (T7) turning inserts after different durations of machining

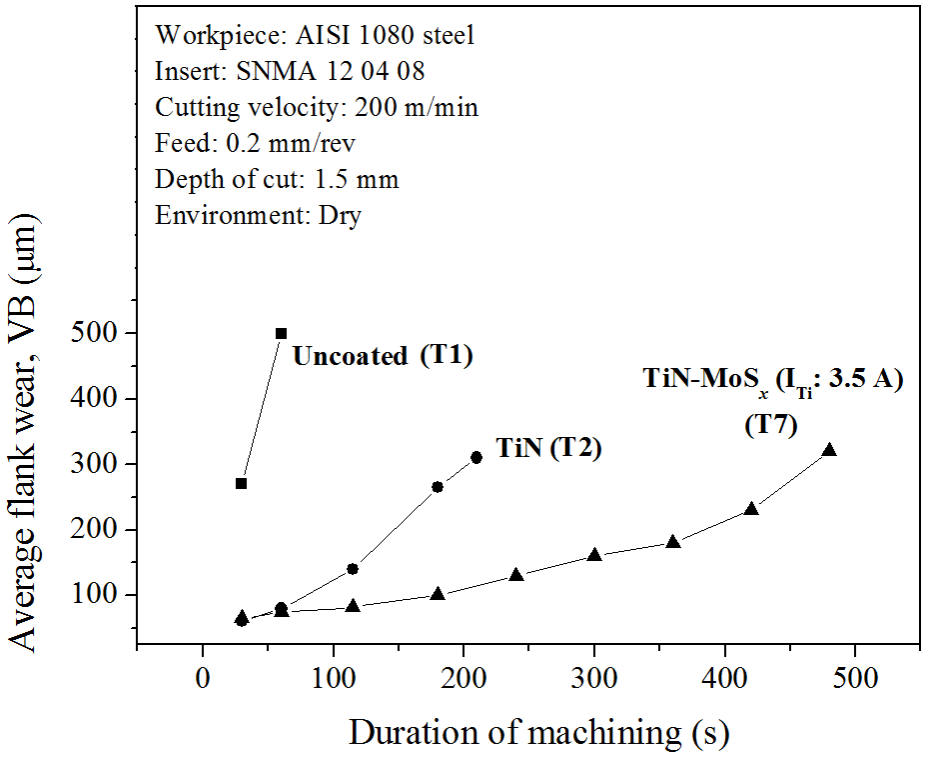

Fig. 10 Variation of average flank wear against machining time for uncoated (T1), TiN coated (T2) and TiN-MoS_x (T7, I_{Ti}: 3.5 A with TiN underlayer) coated WC inserts

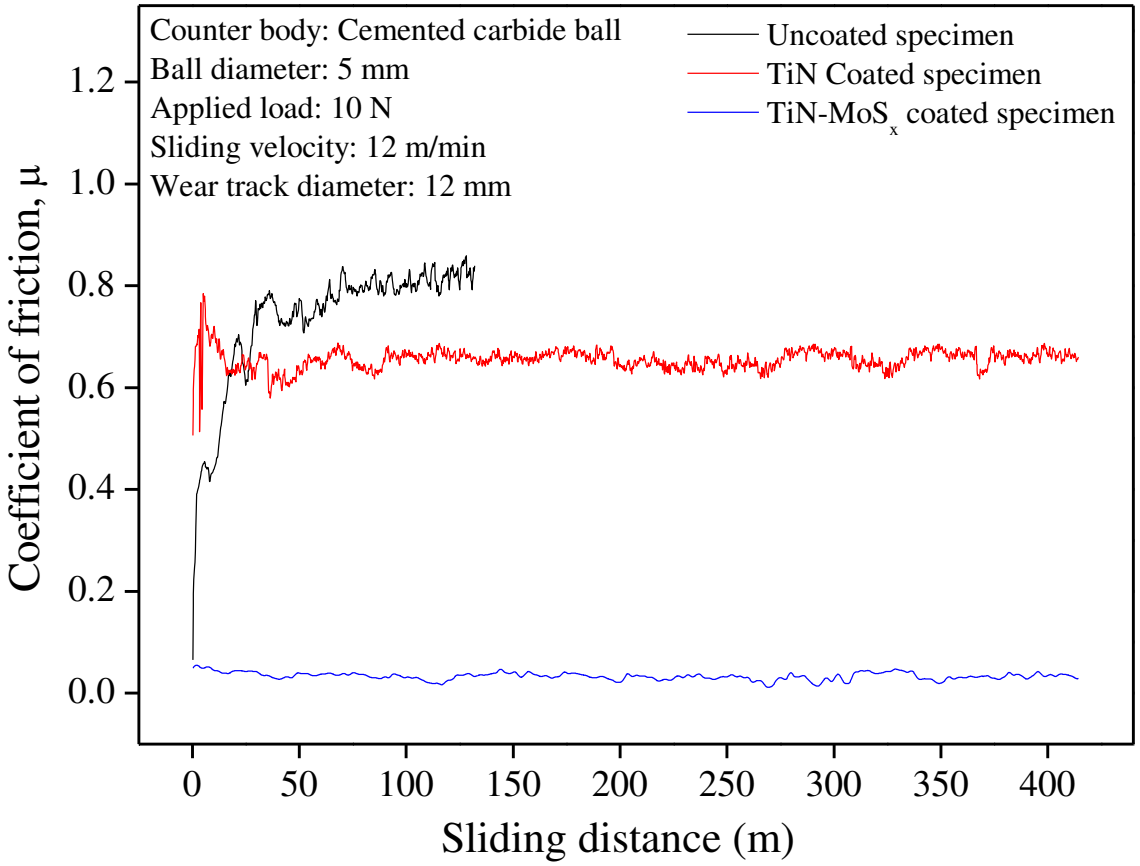

Fig. 11 Coefficient of friction (μ) measured in pin-on-disc test for different coated and uncoated specimens against sliding distance (Gangopadhyay et al (25) and (26))